ELSEVIER

Journal of Nuclear Materials 275 (1999) 324–331

journal of nuclear materials

www.elsevier.nl/locate/jnucmat

Low temperature yield properties of two 7–9Cr ferritic/martensitic steels

P. Spätig[a,*], G.R. Odette[b,c], G.E. Lucas[a,b]

[a] *Department of Chemical Engineering, University of California, Santa Barbara, CA 93106-5080, USA*
[b] *Department of Mechanical and Environmental Engineering, University of California, Santa Barbara, CA 93106-5080, USA*
[c] *Department of Materials, University of California, Santa Barbara, CA 93106-5080, USA*

Received 12 January 1999; accepted 26 April 1999

Abstract

Tensile properties of two 7–9Cr ferritic/martensitic steels have been investigated over the temperature range 77–293 K. Along with the temperature dependence, the strain rate sensitivity of the yield stress has been studied by performing strain rate jump tests. Activation volume and activation energy have been determined and used to identify the rate controlling mechanism of dislocation motion. It has been observed that the temperature and stress dependence of the activation parameters are both consistent with a Peierls mechanism below 190 K. Between 190 and 293 K, other mechanisms begin to operate, replacing the Peierls mechanism. At static strain rates, the athermal regime is reached slightly above room temperature.

PACS: 62.20.Fe; 83.20.Di

1. Introduction

Ferritic/martensitic steels are being considered for use as structural material for the first wall and the blanket structure of fusion reactors due to their good resistance to radiation damage, their low thermal expansion and their high thermal conductivity, [1]. Both structural analysis and safety assessments require a constitutive relation for the temperature and strain rate dependent plastic flow stress and fracture properties. For tensile deformation, the constitutive equation is usually written $\sigma = \sigma(\varepsilon_p, \dot{\varepsilon}_p, T)$, where σ is the flow stress, ε_p and $\dot{\varepsilon}_p$ the plastic strain and the plastic strain rate respectively and T the absolute temperature.

In the path independent formulation, ε_p represents the general 'microstructural state' of the material. More generally, σ depends on the overall microstructure changes induced by effects of irradiation and thermal exposures as well as strain. As part of a longer effort on deformation and fracture in ferritic/martensitic steels, one goal is to characterize the unirradiated low to intermediate temperature constitutive equation for the low activation F82H steel, Fe–8Cr–2W–V–Ta and a modified Fe–9Cr–1Mo–V–Nb steel with quenched and tempered martensitic microstructures. This paper focuses on the low strain regime near yield but post yield constitutive behavior will be presented in a future publication. This study also demonstrates techniques whereby multiple data points can be obtained from a single specimen, a characteristic that is ultimately desirable for irradiation testing where irradiation volume is limited. In particular, the strain rate sensitivity of the stress (SRSS) has been determined by supplementing standard uniaxial tensile tests with both strain rate jumps and stress relaxation experiments at low strains near the yield stress over a range of temperatures. Such procedures avoid performing tests on multiple specimens at different strain rates to determine the SRSS. This information was used to determine the activation volume and energy for the thermally controlled component of the yield stress [2] and to give some physical basis for the

* Corresponding author. Tel.: +1-805 893 3212; fax: +1-805 893 4731.
E-mail address: spatig@engineering.ucsb.edu (P. Spätig)

0022-3115/99/$ - see front matter
PII: S0022-3115(99)00121-X

temperature and strain rate dependence of the flow stress. The activation parameters can be related to the rate controlling processes for dislocation motion and can be used to characterize the temperature range over which they operate. Quantitative descriptions of temperature and strain rate dependence of the yield stress on other structural steels [3,4] are available in the literature. In addition, the effect of irradiation on the dependence of the yield stress has been investigated on different pure bcc metals [5–7] as well as for a mild steel [8] for which the irradiation hardening has been found to be either temperature sensitive or insensitive depending on the test temperature regime. While the evolution of the temperature dependence after irradiation in the low to intermediate temperature regime for the 7–9Cr steel investigated in this paper has yet to be determined, the results presented here constitute a baseline for addressing this issue.

The basis of the thermal activation analysis is presented in Section 2. The experimental procedures are described in Section 3 and the experimental results are reported in Section 4. The constitutive equations for the plastic flow at low to intermediate temperature regime are discussed in Section 5.

2. Thermal activation analysis

The applied uniaxial stress results in a shear stress τ acting on dislocations sufficient to cause plastic shear strain at rate $\dot{\gamma}_p$. In the framework of thermal activation theory, the barriers to dislocation motion are divided into two categories: long range interactions due to large 'obstacles' and short range interactions corresponding to small localized 'obstacles'. The long-range barriers give rise to the microstructure dependent athermal component τ_μ, varying slowly with the dislocation position on its glide plane and weakly dependent on temperature through the shear modulus μ. In contrast, the thermal component τ^* is controlled by short range interactions, which depend on the plastic strain rate ($\dot{\gamma}_p$) and temperature (T). In general both types of barriers are present in the crystal so that the total shear flow stress τ is given by [9]

$$\tau = \tau^*(\dot{\gamma}_p, T) + \tau_\mu(\gamma_p). \tag{1}$$

Assuming a single operative activation mechanism, the deformation process can be described by an Arrhenius equation relating the plastic strain rate to the Gibbs free energy ΔG required by a dislocation to overcome a localized obstacle [10]

$$\dot{\gamma}_p = \dot{\gamma}_{po} \exp\left(-\frac{\Delta G(\tau^*)}{kT}\right), \tag{2}$$

where k is Boltzmann's constant and $\dot{\gamma}_{po}$ is a pre-exponential factor. $\dot{\gamma}_{po}$ accounts for the microstructure, and in particular, is a function of the mobile dislocation density, the mean free dislocation length, the area covered by a dislocation after an activated jump and the Debye frequency. The activation energy is given by (e.g. [11])

$$\Delta G = \Delta g - \tau^* l b X^*, \tag{3}$$

where Δg is the change in the Gibbs free energy due to localized atomic displacement during activation and $\tau^* l b X^*$ the work done by the thermal stress, where l is the average free dislocation segment, b the magnitude of the Burgers vector and X^* the activation distance between the saddle-point position and the equilibrium position of the dislocation in front of the 'obstacle'. The activation volume of the process is defined by

$$V = -\left.\frac{\partial \Delta G}{\partial \tau}\right|_T. \tag{4}$$

Schoeck [11] has shown that $V = lbX^*$. In this paper, the activation volumes are expressed in terms of b^3, where b is the magnitude of the Burgers vector of the a/2⟨1 1 1⟩ dislocation; b is taken to be 2.68 Å. Assuming that $\dot{\gamma}_{po}$ and τ_μ do not vary significantly during a stress and strain rate increment, V can be expressed as

$$V = kT\left(\frac{\partial \ln(\dot{\gamma}_p/\dot{\gamma}_{po})}{\partial \tau}\right) \cong kT\left(\frac{\partial \ln \dot{\gamma}_p}{\partial \tau}\right). \tag{5}$$

Thus, V can be related to experimentally accessible relations between $\dot{\gamma}_p$ and τ as

$$V \cong kT\left(\frac{\Delta \ln \dot{\gamma}_p}{\Delta \tau}\right). \tag{6}$$

Eq. (6) allows the experimental estimation of V by changing the strain rate by a known factor (typically one or two orders of magnitude) and measuring the resulting stress increment.

The activation energy can be obtained by integration of the activation volume with respect to the stress:

$$\Delta G = \int_{\tau_p}^{\tau} V \, d\tau, \tag{7}$$

where τ_p is the Peierls effective stress at 0 K. It must be emphasized that Eq. (7) is not strictly valid since V is a partial derivative of ΔG. However, by deriving the correct procedure to determine ΔG by integration of V over τ, Cagnon [12] showed that Eq. (7) holds when the temperature variations of the shear modulus μ are negligible. In this study, the integration of V was carried out for stresses corresponding to a temperature range over which μ varies less than 6% (the values of μ have been taken from Edsinger [13]). Thus, the use of Eq. (7) is a good approximation.

The shear stress which appears in all the previous equations is obtained from the measured uniaxial tensile

applied stress σ by dividing σ by Taylor's factor M, $\tau = \sigma/M$, where M is 3 for bcc structures [14].

3. Experimental procedures

The two alloys investigated in this study were normalized and tempered martensitic steels. A tungsten-stabilized low activation steel, Fe–7.65Cr–2.0W–0.1C–0.18V–0.04Ta, designated F82H was produced by NKK under the sponsorship of JAERI. The heat treatment of F82H steel was: 0.5 h at 1313 K for normalization and 2 h at 1013 K for tempering. The modified vanadium and niobium-stabilized steel, Fe–8.26Cr–0.1C–0.95Mo–0.2V–0.075Nb, was heat treated for 2.5 h at 1343 K for normalization and for 4.75 h at 1038 K for tempering. It is close to the ASTM designation T91. It has been produced by CEA-CEREM-DEM-Grenoble and provided by ECN Nuclear Energy at Petten.

For F82H, tensile testing was performed on round specimens (3 mm diameter, 18 mm gauge length). The mechanical tests were carried out at temperatures ranging from 77–723 K. The low temperature testing (<293 K) was done at the University California, Santa Barbara with a servo-hydraulic MTS machine at constant nominal strain rate of 2×10^{-4} s^{-1}. The tests at high temperature (>293 K) were conducted at the Paul Scherrer Institute in Switzerland with a Schenck RMC100 machine at a constant nominal strain rate of 10^{-3} s^{-1}. The strain rate sensitivity of the flow stress was investigated at the yield stress by single stress relaxation tests at high temperatures (see for instance [15] for a detailed description of the technique) while strain rate jumps were used at low temperatures.

For the modified 9Cr–1Mo–VNb steel, small flat tensile specimens (0.5 mm thick and 9 mm gauge length) were used for tensile testing. The specimens were electro-discharge machined. They were tested with a servo-hydraulic MTS machine at temperatures ranging between 77 and 293 K at a constant nominal strain rate of 2×10^{-4} s^{-1} and the strain rate sensitivity of the yield stress was also investigated by strain rate jumps.

4. Experimental results

4.1. Temperature dependence of the yield stress and strain rate jumps

The temperature dependence of the yield stress, $\sigma_{0.2}$ defined at 0.2% of plastic deformation, is shown in Fig. 1. For F82H steel, previous reported data of Spätig et al. [16] for high temperature (293–723 K) are included on this plot. A strong dependence of $\sigma_{0.2}$ on temperature is observed below room temperature, while at higher temperatures, the dependence is much weaker for the F82H steel. Fig. 2 shows the yield stress normalized by the shear modulus μ for F82H steel. Above room temperature the normalized yield stress is approximately constant; thus the slight decrease of the absolute yield stress at high temperature appears to be largely a consequence of the corresponding decrease of the elastic modulus.

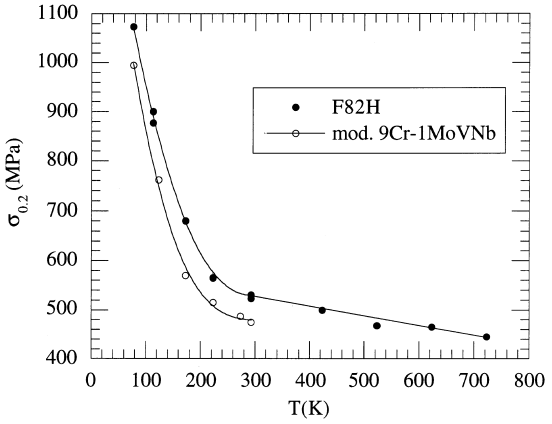

Fig. 1. Temperature dependence of the yield stress of F82H and modified 9Cr–1MoVNb steels.

In order to investigate the strain rate sensitivity of the flow stress, all the low temperature tests (77–293 K) have been supplemented with strain rate jumps at the yield stress. A typical example for F82H, where the strain rate has been increased by two orders of magnitude at 223 K, is presented in Fig. 3. Upward strain rate jump is characterized by positive value of $\Delta\sigma$, which has been systematically measured after the small smooth transient following the strain rate jump as illustrated in Fig. 3. From the strain rate jumps, the corresponding activation volumes have been estimated using Eq. (7).

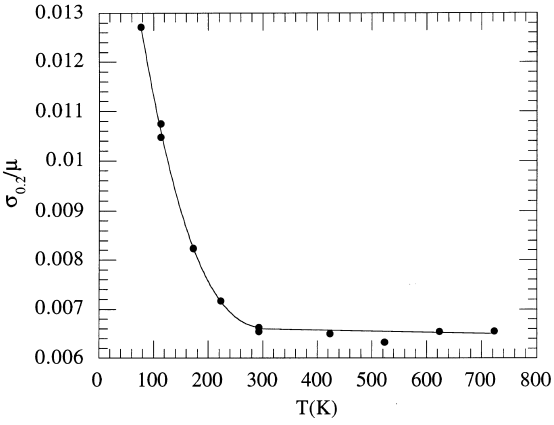

Fig. 2. Temperature dependence of the normalized yield stress of F82H.

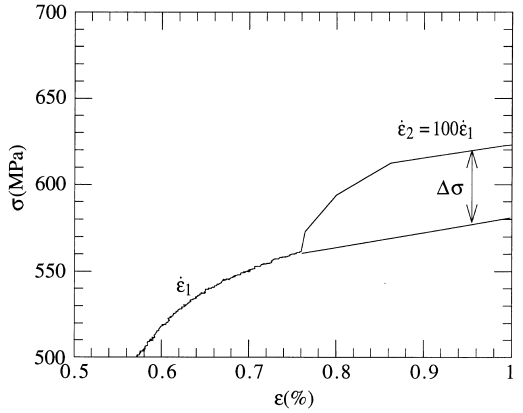

Fig. 3. Example of strain rate jump for F82H at 223 K.

4.2. Activation volume

Fig. 4 presents the stress dependence of the activation volume V at the yield stress for both steels. The open circles and open squares correspond to activation volumes measured by strain rate jumps at temperature $\leqslant 293$ K for modified 9Cr–1Mo–VNb and F82H steels, respectively. The filled squares are activation volume measurements obtained on F82H by stress relaxation for temperature $\geqslant 293$ K previously reported by Spätig et al. [16]. At room temperature, activation volumes obtained from strain rate jump and stress relaxation experiment for F82H are $V(\tau) = 240b^3$ and $V(\tau) = 225b^3$, respectively. Taking account for the experimental uncertainty in the determination of V, which is about 10% for both measurement techniques, the two procedures clearly yield similar activation volume values. At high stress, i.e. in the low temperature regime where $\tau > 200$ MPa $V(\tau)$ is small, typically 10–20b^3. At lower stress or equivalently with increasing temperature, V increases rapidly. This behavior is, of course, consistent with the temperature dependence of the yield stress which reaches the athermal regime where the strain rate sensitivity of the stress disappears and where V becomes very large [16]. The same qualitative behavior is observed for the mod. 9Cr–1MoVNb steel, even though no activation volume measure is available at low stress corresponding to temperatures higher than room temperature.

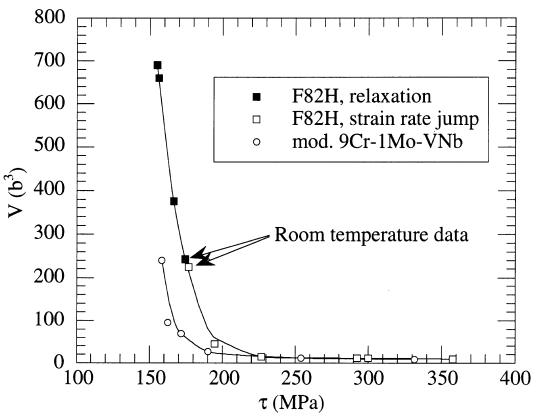

Fig. 4. Stress dependence of the activation volume of F82H and modified 9Cr–1MoVNb steels.

4.3. Activation energy

Eq. (8) has been used to calculate ΔG. Since there is no data below 77 K down to 0 K, the integration must be separated into two contributions as

$$\Delta G = \int_{\tau_p}^{\tau} V\,d\tau = \int_{\tau_p}^{\tau_m} V\,d\tau + \int_{\tau_m}^{\tau} V\,d\tau = \delta G + \int_{\tau_m}^{\tau} V\,d\tau, \quad (8)$$

where τ_p and τ_m are the Peierls stress and the largest measured stress, respectively. Thus, δG corresponds to the high stress and low temperature contribution to ΔG that is not directly measured. However, δG can be estimated by noting that, at a specific $\dot{\gamma}_p$, Eq. (2) indicates that ΔG is a linear function of temperature:

$$\Delta G = kT \ln(\dot{\gamma}_{po}/\dot{\gamma}_p) = \alpha kT, \quad (9)$$

since $\dot{\gamma}_p$ is imposed and $\dot{\gamma}_{po}$ is constant in first approximation. Thus, the activation energy must be zero at 0 K. First, the integration from τ_m to τ yields $\Delta G - \delta G$ represented by the open circles as a function of the stress and temperature in Fig. 5. Then δG is determined by requiring that $\Delta G = 0$ at 0 K. This is schematically shown in Fig. 5. Figs. 6(a) and (b) show the stress and temperature dependence of the activation energy together with the temperature dependence of the yield stress for both steels. As expected from Eq. (9), the temperature dependence of ΔG was found linear with an α of about 24 for F82H and about 29 for modified 9Cr–1Mo–VNb steel. These are typical values for the coefficient α, which are usually of the order of 20–30, e.g. [12,17].

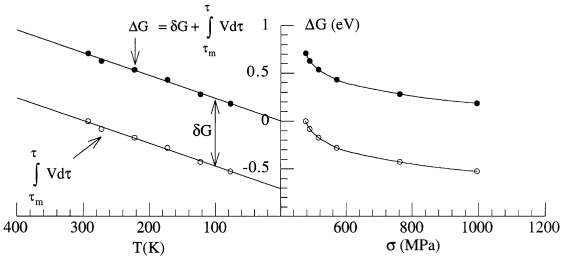

Fig. 5. Schematic representation of the determination of ΔG and δG after integration of V.

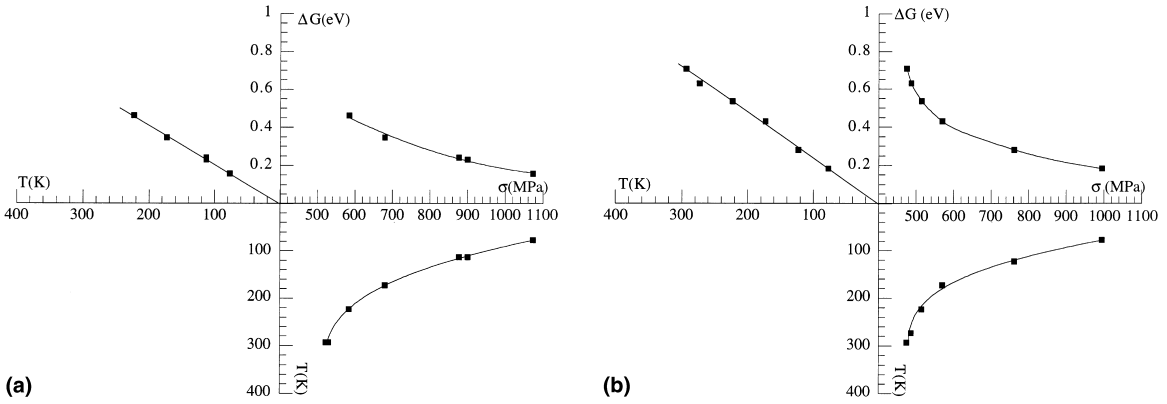

Fig. 6. (a) Stress and temperature dependence of the activation energy along with the temperature dependence of the yield stress: F82H. (b) Stress and temperature dependence of the activation energy along with the temperature dependence of the yield stress: 9Cr–1MoVNb.

5. Discussion

Below room temperature, the yield stress of the steels has been found to be strongly temperature sensitive like other bcc and bcc-like materials. For pure bcc metals, it is well accepted that the low temperature plastic deformation is controlled by an intrinsic frictional force of the Peierls type, opposing the motion of screw dislocation segments, e.g. [18–20]. In the Peierls mechanism, the dislocations experience the periodicity of the lattice as they glide on their slip plane, which results in the presence of peaks and valleys of energy as a function of dislocation position [21]. Different models have been proposed to estimate the energy barrier, but they are all based on the nucleation and propagation of double kinks [22–25], even though they differ in the details. When a double kink is formed on a straight dislocation, mechanical work is done by the stress against the Peierls potential and against the elastic interaction energy between the kinks. The two latter contributions in the energy variation tend to keep the dislocation straight in the Peierls valley. The problem consists in calculating the self elastic energy of the overall kinked dislocation line, for which a theoretical and rigorous treatment has been proposed by Kirchner [26]. However, it requires the solution of an inhomogenous integro-differential equation and more tractable solutions of the problem have been used so far. In the line-tension model (LT model) as proposed by Dorn and Rajnak [24] and Guyot and Dorn [27], the energy is determined by considering the self-interaction of a dislocation line with a double kink described in terms of the dislocation line tension. In the LT model, all the self interaction energy is contained in the energy per unit length, assumed to be independent of the shape of the dislocation. The energy per unit length is assumed to be periodic with the spacing between parallel rows of closely spaced atoms on the slip planes. The double kink energy is then given by the difference between the energy of a kinked dislocation under an effective stress and a straight dislocation under the same stress. However, Seeger [28] showed that the LT model describes accurately the temperature dependence of the yield stress at high and intermediate stress but fails to account for the low stress temperature dependence regime where the long range interaction energy between the kinks should dominate the saddle-energy interaction. Recently, Hollang et al. [29] described the temperature dependence of the yield stress of ultra-high-purity molybdenum single crystals at low temperature by using the LT model at high and intermediate stresses and the elastic kink–kink interaction at low stress. Another approach has been used by Koizumi et al. [25] to estimate the critical energy of a kink-pair formation. Koizumi et al. replaced the continuously curved kinked dislocation by a polygon with a trapezoidal shape, and calculated the interaction energy between the different segments using the existing formulae of Hirth and Lothe [30]. They found that the trapezoid kink pair model is a good approximation of the LT model; in particular, the activation energy of their model reproduces accurately the energy stress dependence of the LT model, except at low stress because the interaction energy of the double kink is not accounted for in the LT model. It is worth mentioning that other models consider the recombination of a critical screw dislocation segment dissociated in a sessile configuration [31–33]. However, it has been pointed out [34] that the recombination model and the double kink nucleation model are two different ways to describe the same lattice effect. For both types of models, the temperature dependence of the flow stress can be obtained by calculating the energy required by the dislocation to overcome the energy barrier as a function of the effective stress and by using the Arrhenius law describing the plastic flow [24,32]. The nature of the rate

controlling mechanism in the low temperature regime for the steels investigated here may be more uncertain than that in pure bcc materials due to the presence of impurities, interstitial elements and small precipitates. It could be argued that these latter features compete or influence the Peierls mechanism. However, the experimental findings support the Peierls mechanism for these steels at low temperature, as outlined below.

Since the LT model usually reproduces well the temperature dependence of the yield stress for bcc metals, except at low stresses, we used the LT model of Dorn and Rajnak [24] to make a comparison between our experimental data and their model. In the following, we adopt the same notation as the original paper of Dorn and Rajnak, where U_k is the formation energy of an isolated kink and U_n is the formation energy of a double kink. The calculations of U_n and U_k show that $2U_k$ is the energy to nucleate a pair of kinks when the effective stress is zero. Dorn and Rajnak derived the temperature dependence of the thermal component of the yield stress as

$$\frac{\tau^*}{\tau_p^*} = f\left(\frac{U_n}{2U_k}\right) \approx f\left(\frac{T}{T_c}\right), \tag{10}$$

where τ_p^* is the Peierls stress, T the temperature and T_c the temperature for which the thermal fluctuations of the lattice with energy $2U_k$ are so frequent that plastic deformation takes place even if τ^* tends to 0. In other words, $2U_k$ is the value of $\Delta G(T_c)$ in our notation, (see Arrhenius law, Eq. (2)). For a given T_c, $2U_k$ or $\Delta G(T_c)$ can be obtained from the plots presented on Figs. 6(a) and (b), where $\Delta G = \alpha kT$. The function f is calculated by Dorn and Rajnak and depends only weakly on the shape of the Peierls barrier considered [27]. We have applied a procedure to superimpose the theoretical curve on the experimental data which is similar to that used by Little for an aluminium-grain-size-controlled mild steel [8]. The procedure consists of determining the two parameters τ_p^* and T_c to obtain a good fit. These parameters as well as $2U_k$ are summarized in Table 1. In Fig. 7, the theoretical curve f, calculated in the case of a pure sinusoidal Peierls hill shape, is presented and the experimental value τ^*/τ_p^* versus T/T_c have been superimposed for both steels. Using these previous parameters, very good agreement with the theoretical curve is obtained up to 210 and 173 K for F82H and modified 9Cr–1Mo–VNb steels, respectively. Given the approximations and uncertainties in the analysis, the difference in the values of T_c is probably not significant and consistent with a nominal T_c for such steels of about 190 ± 20 K. Note that the same behavior was obtained in the mild steel in the study of Little, who showed that the temperature dependence of the yield stress also obeys the predictions of Dorn and Rajnak up to about 195 K. Moreover, there is a rather close correspondence between the values of the Peierls stress, kink energies and T_c for these steels with those found by Little for the mild steel, as shown in Table 1. The fact that the temperature dependence of the yield stress could not be properly described for the low stress regime between 190 and 300 K was also expected and consistent with the LT model for the reasons described above. It can also be argued that above T_c other rate controlling mechanisms are likely to become operative and to compete with the Peierls process. Hence, the interpretation of the temperature dependence of the yield stress between 190 and 300 K becomes more complicated by the fact that several thermally activated mechanisms can be simultaneously active.

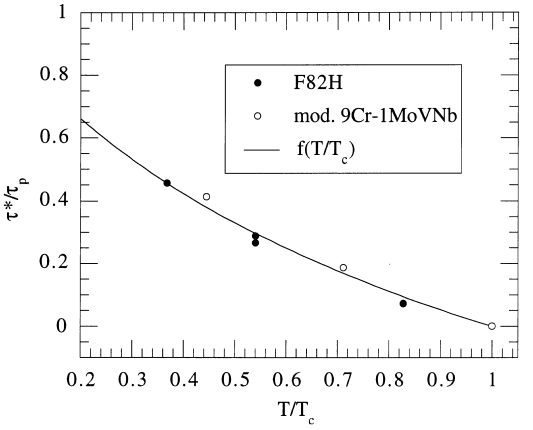

Fig. 7. Effective stress as a function of temperature compared with the theoretical model of Dorn and Rajnak.

Table 1
Parameters used to adjust the experimental data to the model of Dorn and Rajnak. For a consistent comparison, τ_p^* for the mild steel has been recalculated using Taylor's factor equal to 3, as was done for the two other steels and not 2 as in the original paper of Little [8]

	σ_p^* (MPa)	τ_p^* (MPa)	T_c (K)	$2U_k$ (eV)
F82H	1025	342	209	0.43
9Cr–1MoVNb	1025	342	173	0.43
Mild steel Ref. [8]	1230	410	195	0.53

A critical confirmation of the operation of the Peierls process can be obtained by considering the stress dependence of the activation volume because it has been pointed out that mechanisms other than Peierls type could give rise to a similar relation between τ^*/τ_p^* and T/T_c. Dorn and Rajnak also derived the stress dependence of the activation volume. For a sinusoidal energy barrier, they obtained the stress dependence of the activation volume as

$$V\tau_p^*/2U_k = g(\tau^*/\tau_p^*). \tag{11}$$

The previous values of $2U_k$ and τ_p^*, given in Table 1, have been used to plot the experimental data in dimensionless units and they are presented in Fig. 8 along with the theoretical curve. Again a reasonable fit has been found between the experimental data and the theoretical curve. Finally, the small activation volume of the order of 10–20b^3 predicted for the Peierls mechanism, independently of the model, is consistent with the experimental values of V for both steels in this study below 200 K.

While both steels belong to the same class of 7–9Cr ferritic/martensitic steels, they differ with respect to their interstitial, substitutional and impurity levels and small precipitates structures. However, differences in the distribution of such localized obstacles do not affect the rate controlling process of dislocation motion at low temperature. The effect of localized obstacles on the dislocation mobility has been investigated by Guiu [35], who showed that point defects should constitute relatively 'weak' obstacles in bcc structures, owing to the magnitude of the Peierls frictional forces. Provided that the localized obstacle spacing is larger than the critical separation of thermal kinks, Guiu showed that the point defects give rise to an increase of the athermal component but do not modify significantly the rate controlling process. Louchet et al. [36] also developed a model, based on in situ TEM observation of niobium, molybdenum and iron, which accounts for the hardening of localized obstacles in bcc materials. In their model, the motion of screw dislocations is analyzed in terms of a lattice friction along with interaction with localized obstacles. However, at low temperature, the rate controlling process remains the nucleation of double kinks controlled by the average separation of obstacles along the dislocation line. Hence, it is believed that the rate controlling mechanism is little influenced by localized obstacles at low temperature. However, the role of these obstacles is to change the nucleation rate of double kink through the mean free screw dislocation segment length and to modify the athermal component of the stress. Finally, it is worth mentioning that TEM observations on F82H specimens tested at room temperature reveal long screw dislocations with 1/2⟨1 1 1⟩Burgers vector [37].

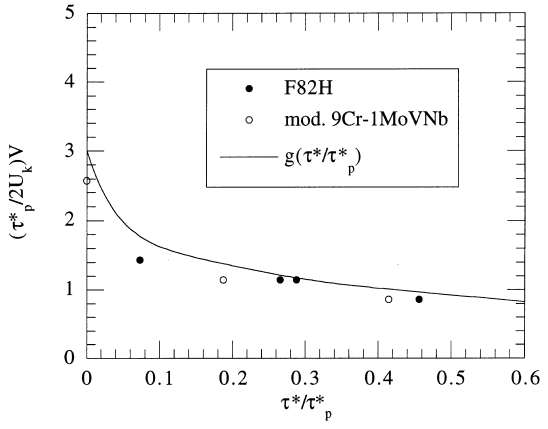

Fig. 8. Activation volume as a function of effective stress compared with the theoretical model of Dorn and Rajnak.

6. Conclusion

Tensile properties of two ferritic/martensitic steels have been studied at low temperatures in the unirradiated condition. In particular, the form of the strain rate and temperature dependence of the yield stress $\sigma_y = \sigma_y(\dot{\varepsilon}_p, T)$ at temperatures below room temperature has been investigated. The strain rate sensitivity of the yield stress has been measured by strain rate jump experiments over the range of temperature (77–293 K). The overall analysis has been done within the framework of thermal activation theory, which allows the determination of thermal activation parameters such as activation volume and activation energy for the rate controlling process of dislocation motion.

It has been shown that the rate controlling process in the low temperature regime is consistent with characteristics of a Peierls-type mechanism. The temperature dependence of the yield stress and the stress dependence of the activation volume agree well with the line-tension model of Dorn and Rajnak. It has been shown that the Peierls mechanism controls the plastic flow below about 190 K. At higher temperatures, the line-tension model appears to no longer agree with the data and it is suggested that other thermally activated processes could become operative and compete with the Peierls mechanism. Above about 300 K, the yield stress is essentially athermal.

Finally, it is emphasized that, by using strain rate jump and stress relaxation experiment, a limited number of specimens have been tested to obtain a relatively large amount of information to describe accurately the constitutive behavior of these steels. This methodology is promising for application to irradiated material, where limited numbers of small specimens are typically available for a given irradiation condition.

Acknowledgements

The financial supports of the Swiss National Science Foundation and of the DOE Office of Fusion Energy, grant No. DE-FG03-94ER54275, are gratefully acknowledged. The technical help of J.W. Sheckherd and D. Gragg for testing of the specimens was greatly appreciated.

References

[1] D.S. Gelles, J. Nucl. Mater. 239 (1996) 99.
[2] A.G. Evans, R.D. Rawlings, Phys. Stat. Sol. 34 (1969) 9.
[3] W. Lei, M. Yao, B. Chen, Eng. Fracture Mech. 53 (4) (1996) 633.
[4] P. Marmy, J.-L. Martin, M. Victoria, Plasma Dev. Oper. 3 (1994) 49.
[5] P. Soo, Trans. AIME 245 (1969) 985.
[6] G.R. Smolik, C.W. Chen, J. Nucl. Mater. 35 (1970) 94.
[7] R.E. Reed, H.D. Guberman, R.W. Armstrong, Phys. Stat. Sol. 37 (1970) 647.
[8] E.A. Little, Phys. Stat. Sol. A 3 (1970) 983.
[9] A. Seeger, J. Diehl, S. Mader, H. Rebstock, Philos. Mag. 2 (1957) 323.
[10] J.W. Christian, B.C. Masters, Proc. Roy. Soc. A 281 (1964) 233.
[11] G. Schoeck, Phys. Stat. Sol. 8 (1965) 449.
[12] M. Cagnon, Philos. Mag. 24 (1971) 1465.
[13] K. Edsinger, PhD thesis, University of California, Santa Barbara, 1995, p. 115.
[14] R.J. Asaro, Advances in Applied Mechanics, vol. 23, Academic Press, New York, 1993, p. 1.
[15] P. Spätig, J. Bonneville, J.L. Martin, Mater. Sci. Eng. A 167 (1993) 73.
[16] P. Spätig, R. Schäublin, S. Gyger, M. Victoria, J. Nucl. Mater. 258–263 (1998) 1345.
[17] J. Diehl, G.P. Seidel, M. Weller, Trans. JIM 9 (1968) 219.
[18] L.P. Kubin, Rev. Deform. Behav. Mater. 1 (1977) 244.
[19] V. Vitek, Cryst. Lattice Def. 5 (1974) 1.
[20] H. Conrad, Acta Metall. 15 (1967) 147.
[21] R. Peierls, Proc. Phys. Soc. 52 (1940) 34.
[22] A. Seeger, Philos. Mag. 1 (1956) 651.
[23] J. Friedel, Dislocations, Pergamon, London, 1964.
[24] J.E. Dorn, S. Rajnak, Trans. AIME 230 (1964) 1052.
[25] H. Koizumi, H.O.K. Kirchner, T. Suzuki, Philos. Mag. A 69 (4) (1994) 805.
[26] H.O.K. Kirchner, Philos. Mag. A 43 (6) (1981) 1393.
[27] P. Guyot, J.E. Dorn, Can. J. Phys. 45 (1967) 983.
[28] A. Seeger, Z. Metallkd. 72 (1981) 369.
[29] L. Hollang, M. Hommel, A. Seeger, Phys. Stat. Sol. A 160 (1997) 329.
[30] J. P. Hirth, J. Loth, Theory of Dislocations, chapter 6 Wiley, New York, 1982.
[31] F. Kroupa, V. Vitek, Can. J. Phys. 451 (1966) 945.
[32] B. Escaig, J. Phys. 28 (1967) 171.
[33] B. Escaig, Phys. Stat. Sol. 28 (1968) 463.
[34] R. Conte, P. Groh, B. Escaig, Phys. Stat. Sol. 28 (1968) 475.
[35] F Guiu, Philos. Mag. 20 (1969) 51.
[36] F. Louchet, L.P. Kubin, D. Vesely, Philos. Mag. A 39 (4) (1979) 433.
[37] R. Schäublin, P. Spätig, M. Victoria, J. Nucl. Mater. 258–263 (1998) 1178.